

Hole-Assisted Few-Mode Multicore Fiber for High-Density Space-Division Multiplexing

Cen Xia, *Student Member, IEEE*, Rodrigo Amezcua-Correa, Neng Bai, *Student Member, IEEE*, Enrique Antonio-Lopez, Daniel May Arrijoja, Axel Schulzgen, Martin Richardson, Jesús Liñares, Carlos Montero, Eduardo Mateo, Xiang Zhou, and Guifang Li, *Senior Member, IEEE*

Abstract—A seven-core few-mode multicore fiber in which each core supports both the LP_{01} mode and the two degenerate LP_{11} modes has been designed and fabricated for the first time, to the best of our knowledge. The hole-assisted structure enables low inter-core crosstalk and high mode density at the same time. LP_{01} inter-core crosstalk has been measured to be lower than -60 dB/km. LP_{11} inter-core crosstalk has been measured to be around -40 dB/km using a different setup. The LP_{11} free-space excitation-induced crosstalk is simulated and analyzed. This fiber allows multiplexed transmission of 21 spatial modes per polarization per wavelength. Data transmission in LP_{01}/LP_{11} mode over 1 km of this fiber has been demonstrated with negligible penalty.

Index Terms—Optical crosstalk, optical fiber communication, optical fiber testing, optical fibers, space division multiplexing.

I. INTRODUCTION

MULTICORE FIBERS (MCF) and few-mode fibers (FMF) are transmission fiber candidates for space-division multiplexing (SDM) [1], [2]. MCFs with lower crosstalk and long-distance transmission in such MCFs have been reported [1], [3]. Transmission in FMFs using up to 5 spatial modes including amplified transmission has also been demonstrated [4]. One of the main goals of SDM is to provide orders of magnitude increase in transmission capacity by increasing the number of space channels. For MCFs demonstrated so far, each core supports only the fundamental mode.

Manuscript received August 1, 2012; revised September 5, 2012; accepted September 11, 2012. Date of publication September 13, 2012; date of current version October 11, 2012.

C. Xia, R. Amezcua-Correa, N. Bai, E. Antonio-Lopez, A. Schulzgen, and M. Richardson are with CREOL, College of Optics and Photonics, University of Central Florida, Orlando, FL 32816 USA (e-mail: cxia@creol.ucf.edu; r.amezcua@creol.ucf.edu; bneng@creol.ucf.edu; enriquelm7@gmail.com; axel@creol.ucf.edu; mcr@creol.ucf.edu).

D. M. Arrijoja is with the Electronics Department, UAM Reynosa Rodhe, Universidad Autónoma de Tamaulipas, Tamaulipas 88779, Mexico (e-mail: daniel_may_arrijoja@hotmail.com).

J. Liñares and C. Montero are with the Faculty of Physics and the School of Optics and Optometry, University of Santiago de Compostela, Santiago de Compostela 15705, Spain (e-mail: suso.linares.beiras@usc.es; carlos.montero@usc.es).

E. Mateo is with the NEC Laboratory America, Princeton, NJ 08540 USA (e-mail: emateo@creol.ucf.edu).

X. Zhou is with the AT&T Labs Research, Middletown, NJ 07748 USA (e-mail: zhoux@research.att.com).

G. Li was with Tianjin University, Tianjin 300072, China. He is now with CREOL, College of Optics and Photonics, University of Central Florida, Orlando, FL 32816 USA (e-mail: li@creol.ucf.edu).

Color versions of one or more of the figures in this letter are available online at <http://ieeexplore.ieee.org>.

Digital Object Identifier 10.1109/LPT.2012.2218801

The number of cores is limited by the desired low crosstalk at sufficiently large core pitch and the maximum fiber cladding diameter (~ 225 microns) from mechanical considerations. The largest number of cores demonstrated for a MCF so far is 19 [5]. Although it is not difficult to increase the number of spatial modes for FMFs, there are some disadvantages associated with FMF with a large number of spatial modes. First, the confinement factor and consequently the bending loss of the higher-order modes will be larger than the lower-order modes. Second, multiplexing and demultiplexing of a large number of modes are complicated and generally introduce more losses. Third, the computational complexity for crosstalk equalization increases with the number of modes. In order to achieve higher capacity for future SDM, the number of spatial channels per fiber needs to be further increased from MCFs and FMFs demonstrated so far. Therefore, the authors have designed and fabricated a few-mode MCF (FMMCF) [6], in which each core supports both the linearly-polarized (LP) LP_{01} mode and the two fold-degenerate LP_{11} modes.

In this letter, we report updated crosstalk measurement of and data transmission in this FMMCF. The inter-core crosstalk values for the LP_{11} and LP_{01} mode are suppressed to be around -40 dB and lower than -60 dB respectively, by a hole-assisted structure around each core. Intra-core modal crosstalk is reduced by designing a large effective index difference between LP_{01} and LP_{11} . This fiber allows SDM transmission of 21 spatial modes per polarization per wavelength.

II. FEW-MODE MULTICORE FIBER

A. Fiber Design

The few-mode MCF was primarily designed to demonstrate both high mode density and ultra-low crosstalk. Theoretically, the crosstalk of a few-mode MCF includes inter-core crosstalk $XT_{LP_{01}}$ and $XT_{LP_{11}}$ for LP_{01} and LP_{11} , and intra-core crosstalk between LP_{01} and LP_{11} . It is known that an effective index difference (Δn_{eff}) larger than 10^{-3} would significantly reduce intra-core crosstalk between the two modes. For inter-core crosstalk, LP_{11} -crosstalk is generally more severe than LP_{01} -crosstalk because the LP_{11} mode is less confined. Therefore the main design goal is to achieve sufficiently low $XT_{LP_{11}}$. It has been demonstrated [3] that the inter-core crosstalk is statistical, obeying the chi-square distribution with mean crosstalk given by

$$XT = 2 \frac{\kappa^2}{\beta} \cdot \frac{R}{D} \cdot L \quad (1)$$

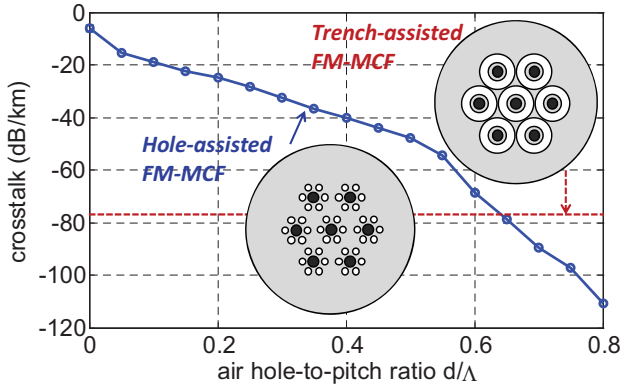


Fig. 1. Inter-core LP_{11} mode crosstalk between two adjacent cores of a hole-assisted few-mode MCF as a function of the air-hole-to-pitch ratio d/Λ as well as that of a trench-assisted few-mode MCF at $\lambda = 1550$ nm.

where κ , β , R , D are the coupling coefficient, propagation constant, bend radius and core pitch, respectively. A large core-to-core distance is a straightforward way to reduce inter-core crosstalk but it would decrease the mode density. Therefore, other than keeping a large core-to-core distance, we applied two approaches to reduce $XT_{LP_{11}}$. First, a hole-assisted structure proposed by ref. [7] has been added outside of each core to improve the mode confinement and hence reduce inter-core crosstalk. This structure has large control flexibility as both the air-hole diameter d and the air-hole pitch Λ can be tuned. A simulation has been conducted shown in Fig. 1 to compare the $XT_{LP_{11}}$ performance between two adjacent cores of this hole-assisted structure and a trench-assisted structure at $\lambda = 1550$ nm [3]. Notice that the center core and outer core would experience 7.8 dB and 4.8 dB higher crosstalk than that shown in Fig. 1 when seven cores are simultaneously excited. The coupling coefficient κ of the LP_{11} mode between two adjacent cores was obtained by calculating the LP_{11} mode profile for this fiber structure using a full-vector finite-element method and substituting it into the following formula [8]

$$\kappa_{12, LP_{11}} = \frac{\omega \epsilon_0 \int_{-\infty}^{+\infty} \int_{-\infty}^{+\infty} (N^2 - N_2^2) \vec{E}_{1, LP_{11}}^* \cdot \vec{E}_{2, LP_{11}} dx dy}{\int_{-\infty}^{+\infty} \int_{-\infty}^{+\infty} \vec{u}_z (\vec{E}_{1, LP_{11}}^* \times \vec{H}_{2, LP_{11}} + \vec{E}_{2, LP_{11}} \times \vec{H}_{1, LP_{11}}^*) dx dy} \quad (2)$$

where N , N_2 are the refractive index distributions of the entire structure and the second waveguide, respectively, \vec{u}_z is the unit vector in z direction. For fair comparison, a typical trench-assisted single-mode multicore fiber in ref. [3] is linearly scaled to a trench-assisted few-mode multicore fiber, which has the same core radius of $6.55 \mu\text{m}$, core index difference 0.36% and core pitch $40 \mu\text{m}$ as the hole-assisted FMMCF in the simulation. The trench index difference, inner cladding radius and the trench width of the scaled trench-assisted FMMCF are -0.55% , $9.8 \mu\text{m}$ and $9.5 \mu\text{m}$ respectively. The air-hole pitch of the hole-assisted FMMCF is $13.3 \mu\text{m}$. It can be seen in the simulation that as the air hole-to-pitch ratio d/Λ increases to above 0.7, or equivalently the air-hole diameter to above $9.3 \mu\text{m}$, the hole-assisted FMMCF starts to outperform the trench-assisted one in terms of low $XT_{LP_{11}}$. Secondly, a large

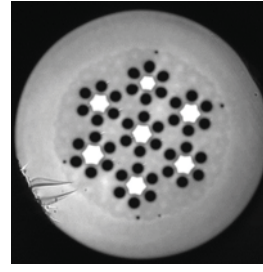


Fig. 2. Cross section of the fabricated FMMCF.

TABLE I
PARAMETERS OF FABRICATED FMMCF

Parameters	Value
Core index difference	0.36%
Core diameter	$13.1 \mu\text{m}$
Core pitch	$40 \mu\text{m}$
Air-hole diameter	$8.2 \mu\text{m}$
Air-hole pitch	$13.3 \mu\text{m}$
Air hole-to-pitch ratio	0.62
Cladding diameter	$192 \mu\text{m}$
Coating diameter	$375 \mu\text{m}$

V-number close to LP_{21}/LP_{02} cut-off condition is selected to better confine LP_{11} mode and reduce inter-core crosstalk without introducing any higher-order modes. With the above design, this novel FMMCF achieves a mode density 8 times larger than a standard single mode fiber (SSMF).

B. Fiber Fabrication and Characteristics

A 1 km fiber was successfully fabricated using the stack-and-draw method. Its cross section and geometry parameters are shown in Fig. 2 and Table I. Because homogeneous MCFs have shown to exhibit lower crosstalk than heterogeneous MCFs with bend-induced coupling, this fiber design is intended to be homogeneous in spite of a slight fabrication size variation from core to core. It should be pointed out that although the fabricated fiber cladding diameter is relatively large, it could be reduced to around $150 \mu\text{m}$ without affecting its transmission properties.

According to the geometric parameters in Table I, the theoretical properties of the MFMCF are listed in Table II. An effective index difference ΔN_{eff} more than 2×10^{-3} is provided between LP_{01} and LP_{11} , as well as LP_{11} and cladding to suppress macro-bending loss. The transmission loss of all modes within 1 km is negligible. The differential group delay (DGD) is measured to be 4.6 ps/m using an interferometric method.

III. CROSSTALK MEASUREMENT

The 1 km FMMCF is wound on a fiber drum with a mandrel radius of 15.9 cm . The LP_{01} and LP_{11} inter-core crosstalk are obtained at $\lambda = 1550 \text{ nm}$. Given a large effective index difference between LP_{01} and LP_{11} , intra-core crosstalk is assumed to be very small. This is also confirmed by an offset-launch impulse response measurement which, after 1 km

TABLE II
SIMULATED AND MEASURED CHARACTERISTICS OF
FABRICATED FMMCF

Fiber Characteristics	LP01	LP11
Measured mode field diameter (MFD) [μm]	11.8	/
Simulated effective area (A_{eff}) [μm^2]	113	170
Simulated cut-off wavelength ^a (λ_c) [nm]	/	$\sim 2100^a$
Simulated chromatic dispersion [ps/nm/km]	23	28
Simulated dispersion slope [ps/nm ² /km]	0.06	0.07
Simulated effective index difference (Δn_{eff})	2.4×10^{-3}	
Measured differential group delay (DGD) [ps/m]	4.6	
Simulated Inter-core crosstalk ^b [dB/km]	-100	-70

^aThe simulated cut-off wavelength for LP_{21}/LP_{02} modes is ~ 1300 nm.

^bInter-core crosstalk is between two adjacent cores.

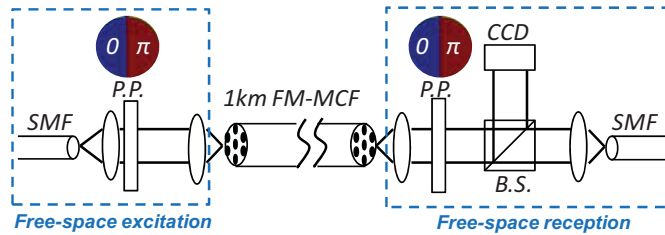


Fig. 3. Schematic setup for LP11 crosstalk measurement.

propagation, only displays two pulses corresponding to the LP_{01} and LP_{11} modes, respectively.

The LP_{01} crosstalk measurement is achieved by using a SSMF butt coupled to the FMMCF for both excitation and reception. This method ensures that no LP_{11} is received even with unintentional offset excitation or intra-core mode coupling. The average measured value of $XT_{LP_{01}}$ is -60 dB, which was limited by the dynamic range of our measurement capability.

In order to measure $XT_{LP_{11}}$, both excitation and reception were conducted in free-space using phase plates shown in Fig. 3. For excitation, light was launched from a SMF into free space and through a phase plate, which has a π phase difference between two semicircles and hence filters out most of the LP_{01} mode. The extinction ratio of the phase plate is estimated to be about 20 dB at 1550 nm. For reception, another phase plate was used to convert LP_{11} mode into LP_{01} so that it can be captured by the receiving SMF and at the same time reject residual LP_{01} mode in the FMMCF if there is any. The free-space excitation at the input FMMCF facet is not a perfect LP_{11} field and thus introduces a discrete crosstalk, which is named excitation-induced crosstalk in this letter. This imperfection is caused by the simple structure of the phase plate with no spatial amplitude modulation and free-space propagation. To simulate this effect, the real field at the input FMMCF facet is calculated by using the following equation:

$$E_o(x_o, y_o) = FT\{A_2(x_2, y_2) \cdot \text{Fresnel}\{P(x_1, y_1) \cdot A_1(x_1, y_1) \cdot FT\{E_i(x_i, y_i)\}\}\} \quad (3)$$

where $E_i(x_i, y_i)$ represents the field of the fundamental mode output from an SMF, $A_1(x_1, y_1)$ and $A_2(x_2, y_2)$ denote the aperture functions of the first and second 20x microscope

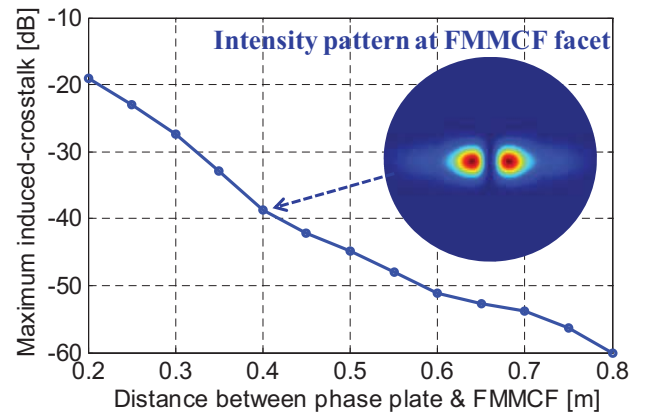


Fig. 4. Simulated LP_{11} free-space excitation-induced crosstalk value as a function of the propagation distance from phase plate to the FMMCF as well as the intensity pattern at FMMCF facet.

objective lens, respectively, $P(x_1, y_1)$ refers to the phase structure of the phase plate, the symbol FT and $Fresnel$ represent Fourier transform and Fresnel diffraction operation. The inset in Fig. 4 shows the calculated intensity pattern at the input FMMCF facet, which contains two tails instead of a clean LP_{11} mode. The excitation-induced crosstalk value varies with the angle with respect to the axis of the phase plate. The excitation is maximum (minimum) for a neighboring core that is placed perpendicular (parallel) to the line dividing the two phases on the phase plate. The maximum excitation-induced crosstalk can be obtained by evaluating the overlap integral between the field at the FMMCF input facet and LP_{01} and LP_{11} mode profiles of the FMMCF. Figure 4 shows that the induced crosstalk also depends on the propagation distance from the phase plate to the FMMCF. Experimental results agree with this trend when the distance between the phase plate and the input FMMCF facet is shorter than 0.5 m, when the crosstalk reaches a floor of about -40 dB for 1 km fiber. The reason might be the simulation does not take account of leaky LP_{21}/LP_{02} modes and cladding modes within the FMMCF. Initially, the measured $XT_{LP_{11}}$ only after a short piece of 2 m fiber and of 1 km fiber were observed to be the same at around -40 dB [6]. As a result, it was concluded that crosstalk floor was due to the measurement setup.

However, we have confirmed recently that the value of -40 dB/km is the actual LP_{11} crosstalk due to the FMMCF itself. This is made possible by adding another step in the $XT_{LP_{11}}$ crosstalk measurement in which one turn of tight bend was introduced near the excitation end of the fiber. The mandrel diameter of the bend is 50 mm. This small amount of tight bend effectively eliminates the leaky LP_{21} mode and cladding modes caused by imperfect excitation. The measured $XT_{LP_{11}}$ after 1 km FMMCF with tight bend is still around -40 dB while that after 2 m fiber is less than -47 dB. These results infer that the detected -40 dB $XT_{LP_{11}}$ is from 1 km of propagation along the fiber. The large discrepancy of $XT_{LP_{11}}$ between experimental measurement and simulation is under investigation. It could be contributed by fiber imperfections, such as the longitudinal variance along the fiber or the hexagonal core shape, which result from the fiber drawing

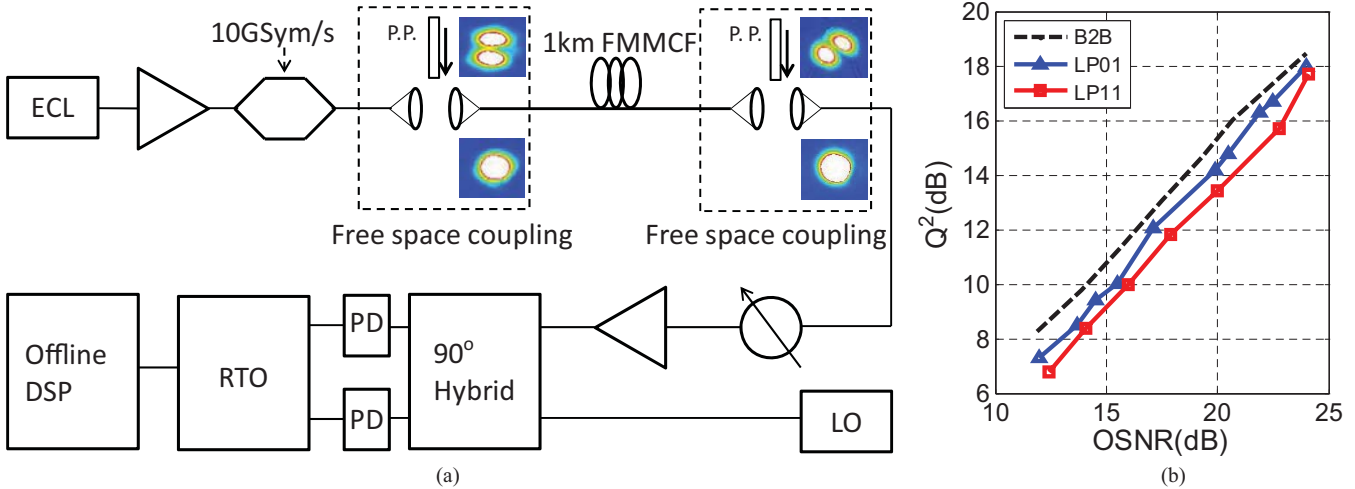


Fig. 5. (a) Setup for LP_{01} and LP_{11} transmissions over 1-km FMMCF. (b) Q_2 factor versus OSNR for back-to-back LP_{01} and LP_{11} transmissions.

process. Another possible reason is that the leaky LP_{21}/LP_{02} mode can act as an intermediary and mediate $XT_{LP_{11}}$ through a considerable intra-core crosstalk with LP_{11} mode. For example, during propagation, a fraction of the launched LP_{11} mode may couple into LP_{21}/LP_{02} mode within the same core, and then the LP_{21}/LP_{02} mode would leak into the modes of the other cores, including LP_{11} modes and be detected as $XT_{LP_{11}}$.

IV. TRANSMISSION EXPERIMENT

The 1km few-mode MCF has been tested in a single channel transmission experiment for both LP_{01} and LP_{11} respectively. The experimental setup is shown in Fig. 5(a) and the fiber was wound on a fiber drum whose mandrel radius is 15.9cm. Light from an external cavity laser at 1550nm is modulated to produce a 10GSym/s BPSK signal using a pattern generator. Then the signal is coupled into either the LP_{01} or LP_{11} mode of an arbitrary core of the 1km FMMCF. Each mode is excited and received in free space with objective lenses for better comparison. The insets in Fig. 5(a) show the LP_{01} and LP_{11} mode profiles at the transmitter and receiver. It is observed that both mode profiles are highly preserved through transmission over the 1 km FMMCF. When LP_{11} is transmitted, one phase plate is added at the input to excite an almost pure LP_{11} mode and another one is inserted at the output to convert the LP_{11} mode back to the LP_{01} mode. The received signal is then sent to a 90 degree hybrid followed by four photo detectors. The variable attenuator and the following amplifier before the hybrid are used for noise loading. The received waveforms were recorded using a real-time oscilloscope and analyzed offline. Fig. 5(b) shows the Q^2 -factors as a function of the optical signal-to-noise ratio (OSNR) for the LP_{01} and LP_{11} modes after transmission as well as for back-to-back measurement. The transmission penalties for the LP_{01} and LP_{11} modes are less than 1dB and 2dB, compared to back-to-back, respectively. These penalties could be due to

discrete mode coupling induced by the imperfect excitation. For example, LP_{11} free-space excitation using a phase plate cannot completely filter out the LP_{01} mode. The residual LP_{01} would transmit together with LP_{11} and produce a small amount of modal dispersion-induced penalty in the LP_{11} transmission experiment.

V. CONCLUSION

A few-mode multicore fiber consisting of 7 cores each supporting 3 spatial modes per polarization has been designed and fabricated. Low core-to-core crosstalk levels have been achieved for both LP_{01} and LP_{11} modes. Data transmission in LP_{01}/LP_{11} mode over 1km of FMMCF has been demonstrated. The 21 degrees of freedom per polarization in this fiber is sufficient to support 1Pb/s transmission in a single fiber.

REFERENCES

- [1] S. Chandrasekhar, *et al.*, "WDM/SDM transmission of 10×128 -Gb/s PDM-QPSK over 2688-km 7-core fiber with a per-fiber net aggregate spectral-efficiency distance product of 40 320 km.b/s/Hz," in *Proc. 37th ECOC*, 2011, pp. 1–2, paper Th.13.C.4.
- [2] N. Bai, *et al.*, "Mode-division multiplexed transmission with inline few-mode fiber amplifier," *Opt. Express*, vol. 20, no. 3, pp. 2668–2680, 2012.
- [3] T. Hayashi, T. Taru, O. Shimakawa, T. Sasaki, and E. Sasaoka, "Design and fabrication of ultralow crosstalk and low-loss multi-core fiber," *Opt. Express*, vol. 19, no. 17, pp. 16576–16592, 2011.
- [4] C. Koebele, *et al.*, "40 km transmission of five mode division multiplexed data streams at 100 Gb/s with low MIMO-DSP complexity," in *Proc. 37th ECOC*, 2011, pp. 1–2, paper Th.13.C.3.
- [5] J. Sakaguchi, *et al.*, "19-core fiber transmission of $19 \times 100 \times 172$ -Gb/s SDM-WDM-PDM-QPSK signals at 305 Tb/s," in *Proc. OFC*, 2012, pp. 1–3, paper PDP5C.1.
- [6] C. Xia, *et al.*, "Hole-assisted few-mode multi-core fiber for high-density space-division multiplexing," in *Proc. IEEE Photon. Summer Topical Meeting 2012*, Seattle, WA, Jul., pp. 206–207, paper TuC4.2.
- [7] K. Saitoh, T. Matsui, T. Sakamoto, M. Koshiba, and S. Tomita, "Multi-core hole-assisted fibers for high core density space division multiplexing," in *Proc. OECC*, 2010, pp. 164–165.
- [8] K. Okamoto, *Fundamental of Optical Waveguides*. New York: Academic, 2006.